Int. J. Heat Mass Transfer. Vol. 31, No. 4, pp. 843–853, 1988
Printed in Great Britain

0017–9310/88 $3.00+0.00
Pergamon Press plc

A frequency response study of packed bed heat transfer at elevated temperatures

M. L. HUBER†
Department of Chemical Engineering and Petroleum Refining, Colorado School of Mines, Golden, CO 80401, U.S.A.

and

M. C. JONES
Center for Chemical Engineering, National Bureau of Standards, Boulder, CO 80303, U.S.A.

(*Received* 30 *March* 1987 *and in final form* 4 *September* 1987)

Abstract—Interphase heat transfer coefficients and effective axial conductivities were obtained for packed beds of uniform alumina spheres with gaseous throughflow in the temperature range 375–1300 K. The method used was parameter estimation from frequency response measurements at two axial locations in a bed when a small sinusoidal temperature disturbance was imparted to the inlet gas temperature. A new model was proposed and frequency response expressions derived in order to take into account the large effective axial conductivity resulting from radiative transfer, unsteady temperature distribution in the solid, and gas–solid interphase heat transfer. A key feature of the model is the use of the local average particle surface temperature as the dependent variable. Results showed that the interphase Nusselt number was independent of temperature but exhibited characteristically low values at low particle Reynolds numbers with a dependence given by

$$Nu = 0.054Re^{1.48}.$$

Effective axial conductivities showed strong temperature dependence typical of radiative transfer. Calculations showed that the observed Reynolds number dependence of the Nusselt number could be partially explained by a microscopic distribution of porosity. These also showed why results with carbon dioxide—a radiatively participating gas—were little different from radiatively non-participating gases.

INTRODUCTION

THE EXCHANGE of heat between a flowing fluid and a fixed bed of particles is a complex process involving several modes of heat transfer and an enormously complex geometry. In general, a geometrically detailed description of the process is both impractical and unnecessary and, instead, it is customary to describe the behavior in terms of a continuum heat balance model. In such a model, averaged values for the dependent variables and global parameters such as conductivities and interphase transfer coefficients are used. Experiments are designed to measure these parameters, often by inference from a comparison of experimental results with model predictions. The hope is that the parameters so obtained reflect the true process on the microscopic scale and can therefore be measured once and for all. The subject has been periodically reviewed [1–4], most recently by Dixon and Cresswell [5]. Our concern in this paper is with heat transfer in packed beds at elevated temperatures with gaseous through flow. While the transmission of radiation through packed beds has received some attention with both experiment and analysis [6–11], the simultaneous exchange of heat with a flowing gas has been neglected. In the work described here, we studied randomly packed beds of uniform ceramic spheres heated by gases at elevated temperatures. The object was to infer values of model parameters as functions of particle Reynolds number, particle size, and temperature under conditions where radiative processes become important.

Previous studies [12–14] indicated that the frequency response technique would be particularly suitable. It has the advantage of eliminating drift problems associated with pulse and step techniques, and has the added potential of permitting the investigation of a broader range of dynamic conditions. Unfortunately, as we found in this work, the range of frequencies experimentally accessible is limited on the high end by one's ability to detect small amplitudes accurately, and on the low end by the need to observe several cycles in a reasonable time. A further compromise was necessitated by the need to approximate an adiabatic bed. An earlier study [15] had shown the importance of maximizing the ratio of heat transmitted axially to that transmitted laterally, and hence lost through the bed walls. When this ratio was too

† Present address: Center for Chemical Engineering, National Bureau of Standards, Boulder, CO 80303, U.S.A.

NOMENCLATURE

a	particle surface area/unit bed volume [m^{-1}]
C	heat capacity [$J\,kg^{-1}\,K^{-1}$]
D	particle diameter [m]
G	transfer function
h	particle–fluid heat transfer coefficient [$W\,m^{-2}\,K^{-1}$]
i	imaginary index
J	objective function
k	thermal conductivity [$W\,m^{-1}\,K^{-1}$]
K_p	Planck mean absorption coefficient
l_m	geometric mean beam length [m]
m	mass flow rate [$kg\,m^{-2}\,s^{-1}$]
M	amplitude ratio
q	heat flux [$W\,m^{-2}$]
r	radial coordinate [m]
R	particle radius [m]
s	Laplace transform variable [s^{-1}]
t	time [s]
T	temperature [K]
V	fluid velocity [$m\,s^{-1}$]
x	axial coordinate [m].

Dimensionless variables

Nu	Nusselt number, hD/k_f
Pe_{eax}	effective axial Peclet number, $C_f\rho_f DV/k_{eax}$
Pe_f	fluid Peclet number, $C_f\rho_f DV/k_f$
Pr	Prandtl number, $C_f\mu/k_f$
Re	Reynolds number, $DV\rho_f/\mu$
W	dimensionless frequency, $\omega D/V$
X	dimensionless axial coordinate, x/D.

Greek symbols

α	thermal diffusivity [$m^2\,s^{-1}$]
ε	bed void fraction
θ	dimensionless surface temperature
μ	viscosity [Pa s]
ρ	density [$kg\,m^{-3}$]
σ	Stefan–Boltzmann constant [$W\,m^{-2}\,K^{-4}$]
ϕ	phase angle [rad]
ω	frequency [$rad\,s^{-1}$].

Subscripts

avg	average over particle volume
b	bed value
c	convective contribution
cd	conductive contribution
e	effective value
eax	effective axial
f	fluid
i	interstitial
p	particle
r	radiative contribution
s	solid, superficial
su	surface of solid
0	reference value.

Superscript

0	stagnant bed value.

Other symbol

—	underline denotes Laplace transformed variable.

low, the axial bed conductivity could not be determined with useful precision. Thus, in the present study, we used as large a bed as possible (12.7 cm in diameter) consistent with reasonable laboratory gas flow rates and electrical power consumption. Bed temperatures ranged between 375 and 1300 K.

In order to carry out frequency response analysis of the experimental results, we had to extend earlier mathematical models to include strong axial conduction resulting from radiative transport. The model is described below and takes as a starting point Gunn's single particle model [16] with centrally symmetric particle temperature distributions. Radiation is accounted for by an effective thermal conductivity in an axial conductive transport equation for the solid phase with particle surface temperature, averaged over the particle surface, as the dependent variable. This is coupled to local intraparticle heat transport through the surface heat flux. In the fluid phase, both accumulation and dispersion are neglected, leaving convection and fluid-to-solid transport.

The results show characteristically low values of Nusselt number at low Reynolds numbers and also show, surprisingly, an insensitivity to strong gas-to-solid radiative transport. These findings are discussed in terms of the well-known fact that porosity is distributed on a microscopic scale in random packed beds [17]. Results are, of course, model dependent, in common with all such techniques of parameter estimation and are offered in that spirit.

EXPERIMENTAL SYSTEM

The experimental method used the frequency response technique, which has been described and used successfully in packed bed heat transfer studies previously [12–14]. It involved generating a sinusoidal temperature disturbance at a known frequency and

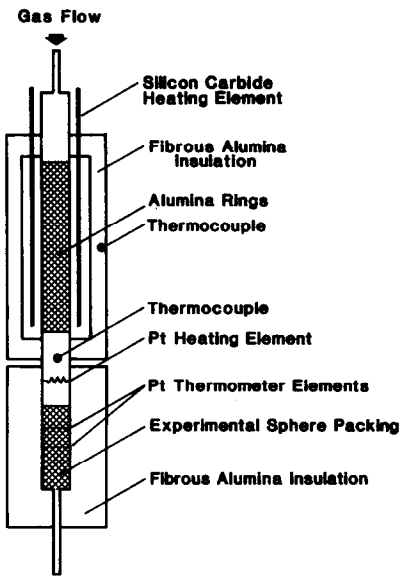

FIG. 1. Diagram of experimental packed bed apparatus.

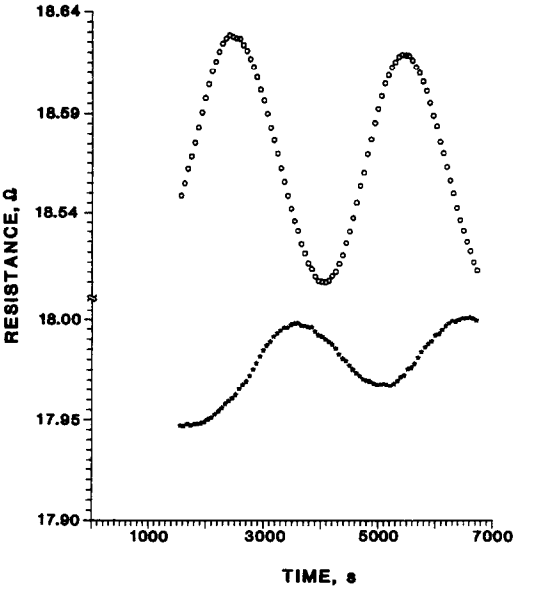

FIG. 3. Typical record of thermometer resistance vs time for upstream and downstream thermometers, respectively.

observing the changes in amplitude and phase as the disturbance propagated down the bed.

A diagram of the apparatus is shown in Fig. 1. Cold gases at a little over atmospheric pressure were heated in a preheater consisting of an alumina tube of 12.7 cm i.d. and 1.52 m in length filled with alumina rings. The tube was surrounded by six silicon carbide heating elements and the entire assembly was encased in lightweight, machineable, fibrous alumina insulation with a 0.40 m o.d. The alumina tube fitted at its lower end directly into the test bed of similar inside diameter of 0.30 m length. The bed assembly was also constructed of concentric cylinders of fibrous alumina insulation to a 0.40 m o.d. The packings consisted of uniform diameter alumina spheres of 3.03, 9.40, 12.73, and 19.82 mm diameter. Void fractions measured by water displacement were 0.39, 0.42, 0.42, and 0.43, respectively.

The gas temperature at the preheater outlet was given a sinusoidal temperature disturbance by the platinum heater element. The resulting perturbation wave in the particle surface temperature was detected by two platinum thermometers shown in Fig. 2. These were in the form of horizontal grids of 0.127 mm diameter, 99.9% pure platinum wire of 0.61 m length wound on thin, square, alumina frames of 8.3 cm

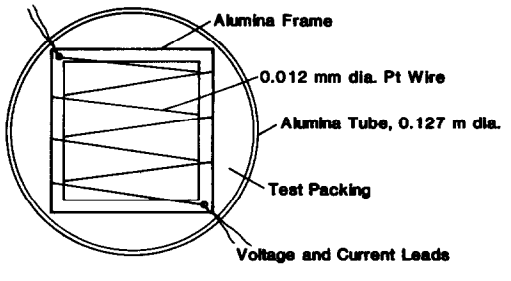

FIG. 2. Platinum thermometer element.

side. These thermometers were placed horizontally at selected heights in the bed packing and were in direct contact with the solid particles and gas. One can show that even with a 50 K temperature difference at the bed inlet, the gas temperature differs by no more than a few millikelvin from the solid at the position of the first platinum thermometer. This is about the limit of precision of the thermometers and thus the error introduced by partial contact with gas is negligible.

The adequacy of the insulation was tested by measuring the amplitude of a 72 K step disturbance superimposed on a gas inlet temperature to the bed of 1058 K. The results indicated that 97% of the energy in the step was transmitted between the grid thermometers; that is, only 3% was lost through the insulation.

To run an experiment, the gas flow was set, the gas temperature at the bed inlet was brought up to the required operating temperature and the sinusoidal perturbation was generated by open loop control from a microcomputer. Observations were made at a minimum of six frequencies for each set of temperature, flow rate, and particle size. Platinum thermometer resistances were measured by a four-wire technique using a digital voltmeter with microvolt accuracy interfaced with the microcomputer. The resulting sine waves were fit to a sinusoid superimposed on a second-degree polynomial to remove small drift voltages, the amplitude and phase being parameters of the fit. A typical record of thermometer resistance for both thermometers is given in Fig. 3. The 95% confidence intervals for the amplitude of the sine waves were 1–2% of amplitude.

MODEL DEVELOPMENT

Several mathematical models have appeared over the years. In the traditional approach, a uniform

superficial velocity (plug flow) is assumed and the model consists of partial differential equations and appropriate boundary conditions expressing the conservation of energy over the solid and fluid phases separately. Exchange between the phases is described in terms of a heat transfer coefficient based on the specific surface area of the packing. In the mathematically more rigorous volume averaging technique, exact equations are derived for volume-averaged solid and fluid temperatures [18, 19]. This method is still under development however, and, for our purposes, a disadvantage is that numerous new parameters are introduced which have not as yet been evaluated. Another disadvantage is that, as currently formulated, equations are not derived in terms of particle surface temperatures which we regard as essential to the expression of radiative transfer and interphase transfer. Thus we preferred the traditional approach.

We chose to represent the radiative contribution to the axial heat flux in terms of an effective conductivity in a solid-phase transient heat conduction equation. While the use of a simplified equation of transfer like the two-flux model [6, 7] would have been more general, here again, more parameters are introduced about which we have little previous knowledge.

Traditional energy balance models may be divided into two categories: discrete and continuous. Among the former, mixing cell models have been studied [20]. These can be extended to take account of radiative exchange between adjacent cells and are in principle simpler to solve than continuous models. Again, however, additional parameters such as view factors and emissivities must be introduced. We have found that, with judicious choice of parameters, such models are capable of matching qualitatively the frequency response curves of continuous models [21], but the reverse process of parameter estimation for all of these parameters would be difficult.

Continuous models may be further subdivided into two groups depending on the treatment of the solid phase. In dispersion-concentric (DC) models [22], the dynamics of the local solid phase are realistically represented by those of a sphere with centrally symmetric temperature profiles. Particle to particle conduction in the solid phase is not considered. Wakao and coworkers [23, 24] compensated for this by introducing excess dispersion in the fluid phase. In continuous solid phase (CS) models [12], the solid phase is treated as a continuum and thermal conduction in the solid phase is permitted, but this at the expense of realistic local particle dynamics: the solid phase temperature is not locally distributed. In both DC and CS models, the partial differential equation for the fluid phase contains a source term for interphase transport.

A final approach which has met with some success and generated a good deal of discussion is due to Vortmeyer and Schaefer [25]. In their model, a single differential equation is derived from the two-phase equations by the simple expedient of equating second derivatives of the solid phase and fluid phase temperatures. Cresswell and Dixon [26] showed that this amounted to equating second moments of the pulse response in the two phases. The result is a single-phase equation containing a dispersion term with a modified dispersion coefficient, a convection term, but no source term from interphase transport. This results in one parameter less to be determined.

For the analysis of frequency response data under conditions of strong radiation, one should consider the following factors. The model must be expressible in terms of the particle surface temperature. It must also take into account the temperature variation within the particles. At low frequencies, the temperature perturbation is transmitted completely into the solid, but as the frequency of the wave is increased, the perturbation in the solid becomes more and more localized at the surface. A rough estimate of the critical frequency can be obtained by setting the dimensionless penetration variable $X = \sqrt{(R^2\omega/\alpha_s)}$ equal to one. For example, with 19.82 mm diameter alumina particles at 1158 K, the critical frequency is approximately 1×10^{-2} rad s^{-1}; above this frequency, non-isothermal effects are important. The experimental data in this study were taken at frequencies where non-isothermal effects are just becoming important. Another important consideration is that if experimental data are obtained at low flow rates, it is necessary to account for axial conduction in the solid phase. Finally, for generality, one should not be restricted to cases where the fluid and solid temperatures are equal.

In view of these requirements, we decided that no single existing model was adequate and that a new model should be developed.

The new model, which we call the extended single particle model (ESPM), considers the solid phase to have an average particle surface temperature distributed in the axial direction. Thus, $T_{su} = T_{su}(x)$. Each particle at axial position x is described in terms of a one-dimensional radial temperature profile: $T_s = T_s(r)$. Conduction and radiation are permitted to occur in the solid phase, but axial conduction and dispersion are neglected in the fluid phase.

Model development for the ESPM begins by writing an energy balance equation for the fluid phase and a local particle energy balance. It is assumed that the properties of the fluid and solid are constants over the range of temperature perturbations of interest, the fluid is in dispersed plug flow, the bed is adiabatic, and the particles are spherical, each with a centrally symmetric temperature distribution.

Fluid

$$\varepsilon\rho_f C_f \frac{\partial T_f}{\partial t} = k_{e,f}\frac{\partial^2 T_f}{\partial x^2} - V\rho_f C_f \frac{\partial T_f}{\partial x} - ha(T_f - T_{su}); \tag{1}$$

Local particle

$$\frac{\partial T_s}{\partial t} = \alpha_s \frac{\partial^2 T_s}{\partial r^2} + \frac{2\alpha_s}{r}\frac{\partial T_s}{\partial r} \tag{2}$$

at $r = 0$, T_s is finite

$$\text{at} \quad r = R, \quad q_p = -k_s \frac{\partial T_s}{\partial r}.$$

At this point the boundary condition on the particle has been left general. The DC model uses a purely convective condition at the particle surface. Instead, consider the flux at the particle surface to arise from not only convective, but also radiative contributions and particle to particle conduction. Furthermore, for small temperature gradients (Siegel and Howell [27]) these modes of transfer may be considered to act in parallel, with no significant interactions. Thus we assume that $\Delta T/T$ is small, so that the flux may be split up into additive radiative, conductive and convective contributions.

To obtain an expression for q_p in terms of the local average fluid and solid surface temperatures, consider a small volume element of a packed bed of width Δx and unit cross-sectional area. An unsteady-state, one-dimensional energy balance on the solid particle phase contained in the volume element leads to

$$(1-\varepsilon)\rho_s C_s \frac{\partial T_{avg}}{\partial t} = -\frac{\partial q_{cd,r}}{\partial x} + h_{c,r} a (T_f - T_{su}) \tag{3}$$

= rate of heat absorption in the solid, per unit bed volume

$= aq_p$.

The term $q_{cd,r}$ is the axial heat flux due to conduction and solid to solid radiation, while $h_{c,r}$ is the local heat transfer coefficient due to convection and gas to solid radiation.

If we define an effective axial bed thermal conductivity by

$$k_{e,b} = \frac{-q_{cd,r}}{\partial T_{su}/\partial x} \tag{4}$$

then equation (3) may be used to write the following boundary condition for a particle at the axial position x:

$$\text{at } r = R, \quad k_s a \frac{\partial T_s}{\partial r} = \frac{-\partial}{\partial x}\left\{-k_{e,b}\frac{\partial T_{su}}{\partial x}\right\} + h_{c,r} a (T_f - T_{su}). \tag{5}$$

FREQUENCY RESPONSE EXPRESSIONS

In this section we develop frequency response expressions for the new model. We now assume that (1) the heat capacity for the fluid is much smaller than that for the solid, so that the thermal capacity of the fluid phase may be ignored, (2) in the presence of strong radiation the axial conduction term in the fluid phase is much smaller than that in the solid phase, and may be neglected. This gives

fluid

$$V\rho_f C_f \frac{\partial T_f}{\partial x} + h_{c,r} a (T_f - T_{su}) = 0; \tag{6}$$

local particle

$$\frac{\partial T_s}{\partial t} = \alpha_s \frac{\partial^2 T_s}{\partial r^2} + \frac{2\alpha_s}{r}\frac{\partial T_s}{\partial r}. \tag{7}$$

The development of the frequency response expressions begins by introducing perturbation variables defined relative to a steady state profile within the bed. The model equations and the local particle boundary conditions are next Laplace transformed and the local particle balance solved for the perturbed particle temperature. This may be evaluated at $r = R$ in order to obtain an equation for the perturbed local particle surface temperature

$$\underline{T}_{su} = \frac{R}{k_s F(s)}\{h_{c,r}(\underline{T}_f - \underline{T}_{su})\} + \frac{k_{e,b}}{a}\frac{d^2 \underline{T}_{su}}{dx^2} \tag{8}$$

where

$$F(s) = \sqrt{\left(\frac{s}{\alpha_s}\right)} R \coth \sqrt{\left(\frac{s}{\alpha_s}\right)} R - 1.$$

This may be solved for the perturbed fluid temperature $\underline{T}_f$ in terms of the average local surface temperature, and differentiated with respect to axial distance. When the resulting two expressions are substituted into the fluid phase balance, and written in dimensionless form, the following third-order ordinary differential equation is obtained for the dimensionless perturbed local particle surface temperature:

$$\frac{d^3\theta}{dX^3} + A_2\frac{d^2\theta}{dX^2} + A_1\frac{d\theta}{dX} + A_0\theta = 0 \tag{9}$$

with coefficients

$$A_2 = 6(1-\varepsilon)Nu/Pe_f$$

$$A_1 = -6(1-\varepsilon)\,Nu\frac{k_f}{k_{e,b}}\frac{2F(s)}{Nu}\frac{k_s}{k_f} + 1$$

$$A_0 = -72(1-\varepsilon)^2 F(s)\frac{Nu}{Pe_f}\frac{k_s}{k_{e,b}}.$$

In equation (9), the particle surface temperature θ has been normalized by the amplitude of the sinusoidally varying fluid temperature at the bed inlet. We have also used $a = 3(1-\varepsilon)/R$ for the specific surface area in beds of spherical particles of radius R.

The solution to this may be cast in the form

$$\theta(X,s) = C_1 e^{\gamma X} + e^{\beta_1 X}\{C_2 e^{\beta_2 X} + C_3 e^{-\beta_2 X}\} \tag{10}$$

$$\beta_1 = -\frac{(a+c)}{2} - \frac{A_2}{3} - \frac{(b+d)i}{2}$$

$$\beta_2 = \frac{\sqrt{3}}{2}[(d-b) + (a-c)i]$$

$$a = \mathrm{Re}\{s_1\}, \quad b = \mathrm{Im}\{s_1\}$$

$$c = \mathrm{Re}\{s_2\}, \quad d = \mathrm{Im}\{s_2\}$$

$$s_1 = [y+(q^3+y^2)^{0.5}]^{1/3}, \quad s_2 = [y-(q^3+y^2)^{0.5}]^{1/3}$$

$$y = \frac{(A_2A_1-3A_0)}{6} - \frac{A_2^3}{27}$$

$$q = \frac{A_1}{3} - \frac{A_2^2}{9}$$

$$\gamma = (s_1+s_2) - \frac{A_2}{3}.$$

It is next necessary to apply some boundary conditions to this differential equation, to determine the constants C_1, C_2, and C_3. Gunn and DeSouza [14] used semi-infinite bed boundary conditions in their analysis of frequency response data; others have also addressed the validity of semi-infinite bed assumptions for finite beds [28, 29]. Observations of the decay of perturbations along the bed in our experiments indicated that the semi-infinite bed boundary condition could easily be applied. We thus take as the outlet boundary condition

$$\text{as } X \to \infty, \quad \theta \to 0. \tag{11}$$

Since the differential equation is third order, two additional boundary conditions are necessary. We chose the case where the temperature perturbation originates in the fluid phase as a reasonable representation of the experiments. At $X = 0$, the perturbation has not yet entered the solid, therefore

$$\text{at } X = 0, \quad \theta = 0. \tag{12}$$

The perturbation is transmitted to the solid via convection and solid to solid radiation. The third boundary condition is obtained from equation (8) with $\underline{T}_{su} = 0$

$$\text{at } X = 0, \quad \frac{d^2\theta}{dX_2} = -6(1-\varepsilon)\,Nu\frac{k_f}{k_{e,b}}. \tag{13}$$

This expresses the fact that the fluid perturbation becomes an energy source for the particle phase, through convection and radiation.

An alternative set of boundary conditions was derived considering the fluid phase perturbation to be immediately transmitted to the solid at the bed entrance, i.e. $\theta = 1$ at $X = 0$. Frequency response calculations showed insensitivity to the choice under the conditions of the experiment.

Upon application of equations (11)–(13), and using the substitution $s = i\omega$, we obtain the frequency response expressions for the ESPM:

$$M = \text{abs}\,(G(i\omega)) = [(\text{Re}\,\{G\})^2+(\text{Im}\,\{G\})^2]^{0.5} \tag{14}$$

$$\phi = \arg\{G(i\omega)\} = \tan^{-1}\frac{\{\text{Im}\,\{G\}\}}{\text{Re}\,\{G\}} \tag{15}$$

where

$$G = e^{\beta_1(X_2-X_1)}\left\{\frac{\sinh(\beta_2X_2)}{\sinh(\beta_2X_1)}\right\}.$$

EXPERIMENTAL RESULTS AND DISCUSSION

Values of the model parameters $k_{e,b}$ and h were obtained by fitting in the frequency domain using nonlinear least square regression. The objective function was the same as that used by Gunn and DeSouza [14]

$$J = \sum\frac{(M_{exp}-M_{calc})^2}{m}. \tag{16}$$

For a typical case with $k_{e,b} = 3.12$ W m^{-1} K^{-1} and $h = 5.11$ W m^{-2} K^{-1}, standard deviations were 0.4 W m^{-1} K^{-1} and 2.4 W m^{-2} K^{-1}, respectively while the residual sum of the squares of the fits were within 0.7% of M. Table 1 gives the results of the fitting procedure. It should be noted that, in the frequency range used, the Vortmeyer–Schaefer model also gave good fits to the amplitude ratio data [21] but this model does not yield separate values for the heat transfer coefficient.

Figure 4 shows the experimental Nusselt numbers plotted against Reynolds number. The data were obtained over a range of temperatures from 600 to 1300 K, but the temperature dependence is weak. This can be seen in Fig. 5 where the Nusselt number has been plotted against temperature for a virtually constant Reynolds number ($6.1 < Re < 7.1$). We note that most data shown are for a non-radiating gas—air—so that temperature effects are only to be expected as a result of temperature dependence of gas properties. The exception is the single datum point for carbon dioxide, but here again the Nusselt number is not exceptional. In Fig. 6, we show the effective stagnant bed thermal conductivities plotted against temperature. These show strong temperature dependence typical of radiation with the effect increasing with particle diameter. Predicted values according to the model of Yagi and co-workers [30, 31] are shown for comparison. Experimental stagnant bed values were obtained by subtracting off a small flow contribution [30, 31] given by

$$k_{eax} - k_e^0 = 0.7Re\,Pr\,k_f.$$

Agreement is not quantitative, but the trends exhibited by the model are certainly correct. Other models such as those of Zehner and Schlünder [32] and Beveridge and Haughey [33, 34] also give acceptable agreement within experimental error.

We wish to draw attention to two points regarding these results. The first has to do with the relationship between Nusselt number and Reynolds number exhibited in Fig. 4. These results are in agreement with the preponderance of data in the literature [1] for small Reynolds numbers. The characteristic slope of 1.48 is somewhat higher than typical, probably due to not separating out particle size as a parameter. The subject has been discussed many times. The point is brought

Table 1. Experimental results

T (K)	D_p (mm)	Re	k_{eax} (W m^{-1} K^{-1})	h (W m^{-2} K^{-1})	Pe_{eax}	Nu
662	3.03	2.17	0.80	1.8	0.094	0.108
819	3.03	1.52	0.90	1.4	0.069	0.071
919	3.03	1.25	1.20	1.6	0.047	0.075
1029	3.03	1.06	0.95	1.1	0.055	0.047
1125	3.03	0.90	1.00	1.0	0.048	0.041
1223	3.03	0.79	0.90	0.8	0.050	0.030
1303	3.03	0.71	1.35	1.2	0.031	0.044
375	9.40	15.4	0.55	5.7	0.604	1.850
608	9.40	6.66	0.55	2.7	0.391	0.548
728	9.40	4.92	1.05	3.1	0.175	0.541
817	9.40	4.06	1.50	3.9	0.111	0.621
903	9.40	3.44	1.35	2.4	0.113	0.353
997	9.40	2.92	1.05	2.9	0.134	0.205
1078	9.40	2.57	1.90	2.0	0.069	0.258
1175	9.40	2.24	1.65	1.6	0.074	0.194
1247	9.40	2.03	1.80	1.5	0.065	0.177
653	12.73	10.7	1.40	5.3	0.261	1.360
758	12.73	8.30	1.50	4.0	0.214	0.915
844	12.73	6.94	1.95	4.5	0.150	0.945
911	12.73	6.12	2.15	4.0	0.127	0.792
1002	12.73	5.23	2.75	5.5	0.092	1.012
1052	12.73	4.83	2.25	3.2	0.108	0.570
1103	12.73	4.48	2.00	4.2	0.117	0.720
1122†	12.73	6.17	2.85	7.2	0.118	1.246
1131	12.73	4.30	2.55	3.0	0.090	0.505
1161	12.73	6.44	3.20	6.5	0.109	1.074
1161	12.73	3.35	1.80	1.8	0.101	0.297
1213	12.73	3.83	1.80	3.2	0.120	0.512
803	19.82	11.7	2.60	5.1	0.183	1.733
856	19.82	10.8	2.75	5.3	0.168	1.710
897	19.82	9.78	2.90	4.4	0.149	1.370
941	19.82	9.26	3.10	4.6	0.137	1.370
1000	19.82	8.39	3.75	6.6	0.108	1.895
1033	19.82	7.95	3.35	3.8	0.117	1.060
1058	19.82	7.46	3.70	4.0	0.102	1.100
1067	19.82	7.36	4.15	3.8	0.090	1.040
1075	19.82	7.45	4.00	4.3	0.095	1.170
1105	19.82	7.12	4.40	4.5	0.085	1.200
1158	19.82	6.60	4.85	4.5	0.074	1.160
1228	19.82	6.00	4.45	3.0	0.077	0.741

† CO_2 data.

out that the minimum value for the Nusselt number should not be less in a packed bed of spheres than it is for an isolated sphere, and thus, the data should be asymptotic to a value of 2.0 at low Reynolds numbers. Opinions have been expressed for this apparent discrepancy: that, in a packed bed, not all the surface of the particle is accessible to the fluid [13] or that neighboring particles shield a given particle from the heat sink [35]; that heat transfer coefficients were estimated using a DC type model in which solid phase axial conduction was not permitted [14]; or that, in the experiments, preferential flow occurred in low-void regions such as are known to exist adjacent to a wall [1, 36]. In the latter case, when measurements are based on a mixed-gas outlet temperature, Martin [36] and Schlünder [1] have shown that the results obtained are to be expected even if, locally, the Nusselt number reached its low-Reynolds number asymptotic value. In this work, strong axial conduction was present but the ESPM model used expressly took this into account. Furthermore, by the way we measured temperatures, the wall effect argument can be eliminated; our thermometers measured particle surface temperature in the core of the bed. When the core mass fluxes were corrrected to allow for preferential flow adjacent to the wall, little change was noted for the smallest spheres used, while, for the larger spheres, the corrections paralleled the trend of the data. This leaves the possibility, implicit in Martin's parallel capillary model, that preferential flow channels may also be found in the core of the bed.

The second point we wish to make is that, in our experiments, both radiating (CO_2) and non-radiating gases (air) were used. Wakao [37] had shown that a radiating gas would have little effect on k_{eax}. In contrast, we had calculated that quite significant differences would be seen in the Nusselt number, all other conditions being equal. To illustrate, the radiative contribution h to the gas–solid heat transfer coefficient can be estimated using the diffuse gray

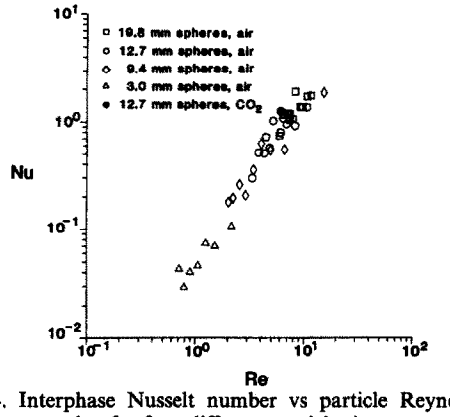

FIG. 4. Interphase Nusselt number vs particle Reynolds number for four different particle sizes.

approximation. Optically thin conditions can be assumed, $K_p \ll 1$, and the mean beam length is the geometric mean beam length, $4\varepsilon/a$. The following expression can then be derived for h_{rad}

$$h_{rad} = \frac{16K_p\varepsilon D\sigma T^3}{6(1-\varepsilon)}. \quad (17)$$

Calculations of the Planck mean absorption coefficient, K_p, have been reported for CO_2 by two methods. At the temperature appropriate for our observations on CO_2, 1122 K, the results of Tien [38] obtained by integration of spectral data give a value of $K_p = 21.3\ m^{-1}$. From total emissivity measurements [39], a corresponding value of $11.5\ m^{-1}$ results. The heat transfer coefficients are 36.5 and 19.7 W m^{-2} K^{-1}, respectively. The experimental result is 7.2 W m^{-2} K^{-1} and is not significantly different from results for air (Fig. 5), however any conclusions drawn from this should be considered tentative pending further experimental study.

We have postulated that these two facts may have the same explanation. We suggest that the observed heat transfer coefficient, when a macroscopic region of the bed is sampled, is lowered from its point value through preferential flow channeling. But we do not consider it likely that preferential flow channels exist

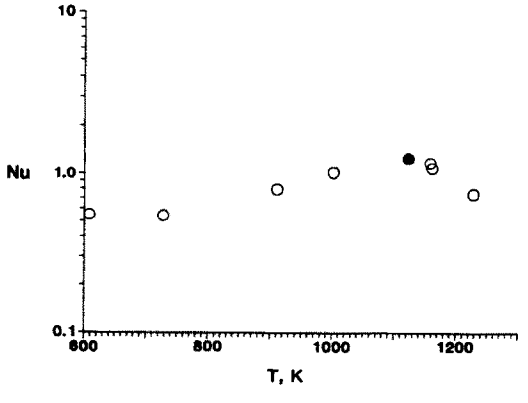

FIG. 5. Interphase Nusselt number vs temperature for the particle Reynolds number range $6.1 < Re < 7.1$. The single filled circle is for carbon dioxide.

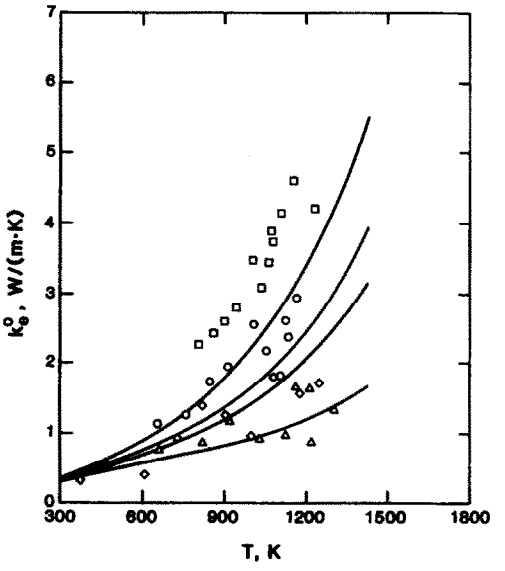

FIG. 6. Effective axial thermal conductivities corrected for stagnant bed conditions compared with the correlation of Yagi and Kunii [30]. The symbols for different particle sizes are the same as in Fig. 4.

on a macroscopic scale since the beds were carefully prepared. Instead, the microscopic distribution of porosity appears to be capable of explaining the apparent lowering of the heat transfer coefficient.

To investigate this hypothesis, we performed calculations using a model with a continuous distribution of porosity. Beveridge and Haughey [17, 40] provide curves for the variation of local mean voidage about a given sphere center in a randomly packed bed of equal size spheres. For ease of calculation the Beveridge and Haughey local void fraction distribution was approximated by a three-parameter gamma distribution of the form

$$f(\varepsilon) = \frac{\lambda^r}{\Gamma(r)}(\varepsilon-u)^{r-1}e^{-\lambda(\varepsilon-u)}, \quad u \leqslant \varepsilon \leqslant \infty \quad (18)$$

$$= 0, \quad \varepsilon < u$$

with parameter values

$$\lambda = 32, \quad r = 3.5, \quad u = 0.28.$$

These values give a mean bed voidage of 0.389 and a standard deviation of 0.05, close to the parameters found by Beveridge and Haughey for loose packed beds.

For a fixed value of frequency, particle diameter and temperature, we chose a reference interstitial velocity V_{i0} at some reference void fraction ε_0. If it is assumed that the interstitial velocity varies as the square of the mean hydraulic diameter then, for a bed of spheres

$$V_s(\varepsilon) = \varepsilon\left(\frac{\varepsilon}{1-\varepsilon}\right)^2\left(\frac{1-\varepsilon_0}{\varepsilon_0}\right)^2 V_{i0}. \quad (19)$$

The reference velocity was chosen and a local Nusselt number calculated from a single particle correlation.

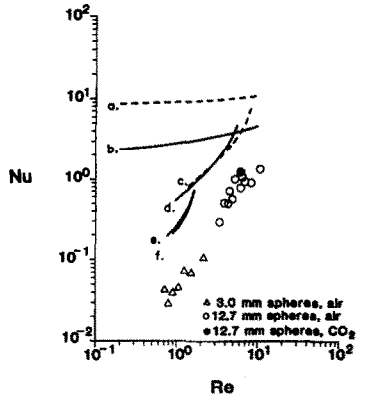

FIG. 7. Comparison of experimental interphase Nusselt numbers with calculations showing the effect of a porosity distribution: (a) single particle correlation of Ranz [41] for CO_2 with additional contribution for radiative transfer; (b) Ranz correlation; (c) distributed porosity calculation for CO_2, 12. 7 mm spheres, 1122 K, $L/D = 4$; (d) as for (c) with air, 1053 K; (e) 3.0 mm spheres with air, 1019 K, $L/D = 12$; (f) as for (e), $L/D = 8$.

We chose, for purposes of illustration, the single particle correlation of Ranz [41]. For CO_2, the additional radiative contribution by equation (17) was added. The amplitude and phase of the temperature perturbation were then functions of $V_s(\varepsilon)$ and, for a given value of ε, $\theta(iw)$ could be calculated using the ESPM model. An average value for the packed bed was found using the weighted average at each of the two thermometer positions

$$\langle\theta(iw)\rangle = \int_0^\infty \theta(iw, \varepsilon) f(\varepsilon)\, d\varepsilon. \tag{20}$$

Similarly, we found the average superficial velocity and void fraction

$$\langle V_s\rangle = \int_0^\infty V_s(\varepsilon) f(\varepsilon)\, d\varepsilon \tag{21}$$

$$\langle\varepsilon\rangle = \int_0^\infty \varepsilon f(\varepsilon)\, d\varepsilon. \tag{22}$$

The amplitude ratio from equation (20) was then compared with that from equation (15) for a uniform porosity bed with the same average velocity and void fraction in order to find the value of Nusselt number which gave the same amplitude ratio. This was repeated for new choices of reference velocity. Sample results are shown in Fig. 7.

The distributed porosity model, while not being in precise agreement with the experimental data, does show the correct trend with Reynolds number and the insensitivity to the additional radiative contribution observed for the CO_2 case. However, certain shortcomings of the model should be pointed out. The most serious is that the enhancement of velocity in regions of higher porosity according to equation (19) is overestimated since we have tacitly assumed that the local pressure gradient is equal to the value it would have if the medium were a structureless continuum and the interconnection of flow passages ignored. Ng and Payatakes [42] have demonstrated this fact by comparison with a random network model. Our model also neglects the thermal interaction between adjacent regions of differing porosity.

Thus we conclude that, while a distributed porosity model is an improvement over uniform porosity for predicting the dynamics of packed bed heat transfer, further developments in models need still to be made. The results are, nevertheless, encouraging.

CONCLUSIONS

(1) We have introduced a new model, the extended single particle model, which allows for axial conduction in the solid, particle–particle and gas–particle radiative transfer, and intraparticle temperature gradients. Frequency response expressions for this model were developed, and used to obtain experimental values for the heat transfer parameters: gas particle heat transfer coefficient and the effective thermal conductivity of the packed bed. The model is useful for packed beds subject to high temperatures and low fluid flow rates.

(2) We obtained experimental values for Nusselt number in the Reynolds number range 0.7–16, which were found to follow the relation

$$Nu = 0.054 Re^{1.48}.$$

The data showed a decreasing Nusselt number with decreasing Reynolds number, with no asymptotic limit apparent. A distribution of porosity in the bulk of the bed could be responsible for some of the observed depression of Nusselt numbers. Future model development should take into account this distribution of porosity.

(3) We obtained experimental values of the effective axial thermal conductivity. These data showed a strong dependence on temperature, increasing with particle diameter. They were compared with several correlations for k_e^0 available in the literature and found to be in general agreement.

Acknowledgements—This work was supported by the United States Department of Energy under Contract # DE-AC01-81E10823.

REFERENCES

1. E. U. Schlünder, Transport phenomena in packed beds reactors, Chemical Reaction Engineering Reviews—Houston, 111–159, American Chemical Society (1978).
2. A. G. Dixon and D. L. Cresswell, Theoretical prediction of effective heat transfer parameters in packed beds, *A.I.Ch.E. Jl* **25**, 663–676 (1979).
3. A. R. Balakrishnan and D. C. T. Pei, Heat transfer in gas–solid packed bed systems—a critical review *I&EC Proc. Des. Dev.* **18**, 30–50 (1979).

4. N. Wakao, S. Kaguei and B. Shiozawa, Effect of axial fluid thermal dispersion coefficient on Nusselt number of dispersion concentric model of packed beds at low flow rates, *Chem. Engng Sci.* **32,** 451–454 (1977).
5. A. G. Dixon and D. L. Cresswell, Effective heat transfer parameters for transient packed-bed models, *A.I.Ch.E. Jl* **32,** 809–819 (1986).
6. H. C. Hamaker, Radiation and heat conduction in light-scattering material, *Philips Res. Rep.* **2,** 103–111 (1947).
7. J. C. Chen and S. W. Churchill, Radiant heat transfer in packed beds, *A.I.Ch.E. Jl* **9,** 35–41 (1963).
8. G. Flamant, Theoretical and experimental study of radiant heat transfer in a solar fluidized-bed receiver, *A.I.Ch.E. Jl* **28,** 529–535 (1982).
9. C. K. Chan and C. L. Tien, Radiative transfer in packed spheres, *J. Heat Transfer, ASME* **96,** 52–58 (1974).
10. Y. S. Yang, J. R. Howell and D. E. Klein, Radiative transfer through a randomly packed bed of spheres by the Monte Carlo method, *J. Heat Transfer, ASME* **105,** 325–332 (1983).
11. M. Q. Brewster and C. L. Tien, Radiative transfer in packed fluidized beds: dependent versus independent scattering, *J. Heat Transfer, ASME* **104,** 573–579 (1982).
12. H. Littman, R. Barile and A. Pulsifer, Gas–particle heat transfer coefficients in packed beds at low Reynolds numbers, *I&EC Fund.* **7,** 554–560 (1968).
13. H. Littman and D. E. Sliva, Gas–particle heat transfer coefficients in packed beds at low Reynolds numbers, 4th International Heat Transfer Conference, Paris, Vol. 7, pp. 1–11 (1970).
14. D. J. Gunn and J. F. C. DeSouza, Heat transfer and axial dispersion in packed beds, *Chem. Engng Sci.* **29,** 1364–1371 (1974).
15. S. Skaff, High temperature heat transport in porous media—apparatus design and testing, Master's Thesis, T-2432, Colorado School of Mines (1981).
16. D. J. Gunn, The transient and frequency response of particles and beds of particles, *Chem. Engng Sci.* **25,** 53–66 (1970).
17. G. S. G. Beveridge and D. P. Haughey, Local voidage variation in a randomly packed bed of equal spheres, *Chem. Engng Sci.* **21,** 905–916 (1966).
18. S. Whitaker, Radiant energy transport in porous media, *Ind. Engng Chem. Fund.* **19,** 210–218 (1980).
19. J. Levec and R. G. Carbonell, Longitudinal and lateral thermal dispersion in packed beds, Part I: theory, *A.I.Ch.E. Jl* **31,** 581–590 (1985).
20. J. Votruba and V. Hlavacek, Steady state operation of fixed bed reactors and monolithic structures. In *Chemical Reactor Theory—a Review*. Prentice-Hall, Englewood Cliffs, New Jersey (1977).
21. M. L. Huber, An investigation of heat transfer in packed beds at high temperatures and low Reynolds number, Ph.D. Thesis, T-2912, Colorado School of Mines (1985).
22. S. Kaguei, B. Shiozawa and N. Wakao, Dispersion concentric model for packed bed heat transfer, *Chem. Engng Sci.* **32,** 507–513 (1977).
23. N. Wakao, Particle-to-fluid transfer coefficients and fluid diffusivities at low flow rate in packed beds, *Chem. Engng Sci.* **31,** 1115–1122 (1976).
24. N. Wakao, S. Kaguei and B. Shiozawa, Effect of axial fluid thermal dispersion coefficient on Nusselt numbers of dispersion-concentric model of packed beds at low flow rates, *Chem. Engng Sci.* **32,** 451–454 (1977).
25. D. Vortmeyer and R. J. Schaefer, Equivalence of one- and two-phase models for heat transfer processes in packed beds: one dimensional theory, *Chem. Engng Sci.* **29,** 485–491 (1974).
26. D. L. Cresswell and A. G. Dixon, Reply to comments by Vortmeyer and Berninger on the paper "Theoretical prediction of effective heat transfer parameters in packed beds," *A.I.Ch.E. Jl* **28,** 511–513 (1982).
27. R. Siegel and J. Howell, *Thermal Radiation Heat Transfer*. Hemisphere, New York (1981).
28. N. Wakao and S. Kaguei, Validity of infinite bed assumption in input-response heat transfer measurements, *Chem. Engng Sci.* **37,** 1819–1821 (1982).
29. D. J. Gunn, Theory of axial and radial dispersion in packed beds, *Trans. Instn Chem. Engrs* **47,** T351–T359 (1969).
30. S. Yagi and D. Kunii, Studies on effective thermal conductivities in packed beds, *A.I.Ch.E. Jl* **3,** 373–381 (1957).
31. S. Yagi, D. Kunii and N. Wakao, Studies on effective thermal conductivities in packed beds, *A.I.Ch.E. Jl* **6,** 543–546 (1960).
32. P. Zehner and E. U. Schlünder, Warmeleitfahigkeit von Schluttungen bei mabingen temperaturen, *Chemie-Ingr-Tech.* **42,** 933–941 (1970).
33. G. S. G. Beveridge and D. P. Haughey, Axial heat transfer in packed beds. Stagnant beds between 20 and 750°C, *Int. J. Heat Mass Transfer* **14,** 1093–1113 (1971).
34. G. S. G. Beveridge and D. P. Haughey, Axial heat transfer in packed beds. Gas flow through beds between 20 and 650°C, *Int. J. Heat Mass Transfer* **15,** 953–968 (1972).
35. A. R. H. Cornish, Note on minimum possible rate of heat transfer from a sphere when other spheres are adjacent to it, *Trans. Instn Chem. Engrs* **43,** T332–T333 (1965).
36. H. Martin, Low Peclet number particle-to-fluid heat and mass transfer in packed beds, *Chem. Engng Sci.* **33,** 913–919 (1978).
37. N. Wakao, Effect of radiating gas on effective thermal conductivity of packed beds, *Chem. Engng Sci.* **28,** 1117–1118 (1973).
38. C. L. Tien, Thermal radiation properties of gases, *Adv. Heat Transfer* **5,** 315 (1968).
39. W. H. McAdams, *Heat Transmission*. McGraw-Hill, New York (1964).
40. G. S. G. Beveridge and D. P. Haughey, Local property variations in a randomly packed bed of equal sized spheres, *Chem. Engng Sci.* **22,** 715–718 (1967).
41. W. E. Ranz, Friction and transfer coefficients for single particles and packed beds, *Chem. Engng Prog.* **48,** 247–253 (1952).
42. K. M. Ng and A. C. Payatakes, Critical evaluation of the flow rate–pressure drop relation assumed in permeability models, *A.I.Ch.E. Jl* **31,** 1569–1571 (1985).

ETUDE DE LA REPONSE EN FREQUENCE DU TRANSFERT THERMIQUE D'UN LIT FIXE A HAUTE TEMPERATURE

Résumé—Des coefficients de transfert de chaleur interphase et des conductivités axiales effectives sont obtenues pour des lits fixes de sphères uniformes d'alumine avec traversée de gaz pour un domaine de température de 375 à 1300 K. La méthode utilisée est l'estimation paramétrique à partir des mesures de réponse en fréquence en deux points sur l'axe du lit avec une petite perturbation sinusoïdale de température à l'entrée du gaz. On prend en compte la grande conductivité axiale effective qui résulte du transfert radiatif, de la distribution instable de température dans le solide, et du transfert thermique à l'interface gaz–solide. Les résultats montrent que le nombre de Nusselt est indépendant de la température mais que de faibles valeurs correspondent aux petits nombres de Reynolds de la particule avec la dépendance

$$Nu = 0{,}054Re^{1{,}48}.$$

Les conductivités axiales effectives montrent une forte dépendance à la température typique du transfert radiatif. Les calculs montrent que la dépendance observée au nombre de Reynolds du nombre de Nusselt peut être partiellement expliquée par une distribution microscopique de porosité. Ils montrent aussi que les résultats avec le dioxyde de carbone—un gaz rayonnant—sont peu différents de ceux pour des gaz transparents.

FREQUENZGANGUNTERSUCHUNG BEI DER WÄRMEÜBERTRAGUNG IN SCHÜTTUNGEN BEI ERHÖHTER TEMPERATUR

Zusammenfassung—Es wurden Wärmeübergang und effektive axiale Wärmeleitfähigkeit in einer gasdurchströmten Schüttung aus gleich großen Aluminiumkugeln in einem Temperaturbereich von 375 bis 1300 K ermittelt. Diese Größen wurden durch Parameterabschätzung aus Frequenzgangmessungen an zwei hintereinander liegenden Stellen in der Schüttung bestimmt, wobei der Gaseintrittstemperatur eine kleine sinusförmige Temperaturstörung aufgeprägt wurde. Es wird ein neues Modell vorgestellt, und Frequenzgangfunktionen wurden abgeleitet, um die große effektive axiale Wärmeleitfähigkeit zu berücksichtigen, die vom Strahlungsaustausch, von der instationären Temperaturverteilung und vom Wärmeübergang herrührt. Eine Besonderheit des Modells ist die Verwendung von örtlichen mittleren Partikeloberflächentemperaturen als abhängige Variable. Die Nusselt-Zahl ist unabhängig von der Temperatur, erreicht aber kleine Werte, wenn die Reynolds-Zahl der Partikel klein ist. Es gilt $Nu = 0{,}054Re^{1{,}48}$. Die effektive Längswärmeleitfähigkeit zeigt eine für Strahlungsaustausch typische starke Temperaturabhängigkeit. Berechnungen zeigen, daß die beobachtete Abhängigkeit der Nusselt-Zahl von der Reynolds-Zahl teilweise durch eine mikroskopische Porositätsverteilung erklärt werden kann. Sie zeigen auch, warum Ergebnisse mit Kohlendioxid (einem am Strahlungsaustausch beteiligten Gas) sich nur wenig von solchen mit nicht am Strahlungsaustausch beteiligten Gasen unterscheiden.

ИССЛЕДОВАНИЕ ЧАСТОТНОЙ ХАРАКТЕРИСТИКИ ТЕПЛООБМЕНА ПЛОТНОГО СЛОЯ ПРИ ПОВЫШЕННЫХ ТЕМПЕРАТУРАХ

Аннотация—Коэффициенты межфазного теплообмена и эффективные коэффициенты продольной теплопроводности получены для плотных слоев однородных алюминиевых шариков при обтекании их потоком газа с температурой от 375 до 1300 К. Используемый метод представлял собой оценку параметров на основе измерений частотной характеристики в двух точках по оси слоя с небольшими синусоидальными возмущениями температуры газа на входе. Предложена новая модель и выведены выражения для частотных характеристик с целью учета высокой эффективной продольной теплопроводности как следствия радиационного теплообмена, нестационарного распределения температуры в твердых частицах и межфазного (газ–твердые частицы) теплообмена. Основной особенностью модели является использование локальной средней температуры поверхности частиц как зависимой переменной. Результаты показали, что число Нуссельта для межфазного теплообмена было независимым от температуры, но продемонстрировали низкие значения его при небольших величинах числа Рейнольдса (для частиц) в соответствии с зависимостью, представленной как $Nu = 0{,}054Re^{1{,}48}$. Эффективные коэффициенты продольной теплопроводности сильно зависят от температуры, что характерно для радиационного теплопереноса. Расчеты показывают, что наблюдаемая зависимость числа Нуссельта от числа Рейнольдса может быть отчасти объяснена наличием микроскопической пористости. Это также объясняет тот факт, что результаты опытов, проведенных с двуокисью углерода (излучательно активный газ), мало отличались от данных, полученных с излучательно неактивными газами.